

UCLA

UCLA Previously Published Works

Title

Non-integer temporal exponents in trans-interface diffusion-controlled coarsening

Permalink

<https://escholarship.org/uc/item/56f6b1x4>

Journal

Journal of Materials Science, 51(13)

ISSN

0022-2461

Author

Ardell, Alan J

Publication Date

2016-07-01

DOI

10.1007/s10853-016-9953-0

Peer reviewed

Non-integer temporal exponents in trans-interface diffusion-controlled coarsening

Alan J. Ardell

Journal of Materials Science

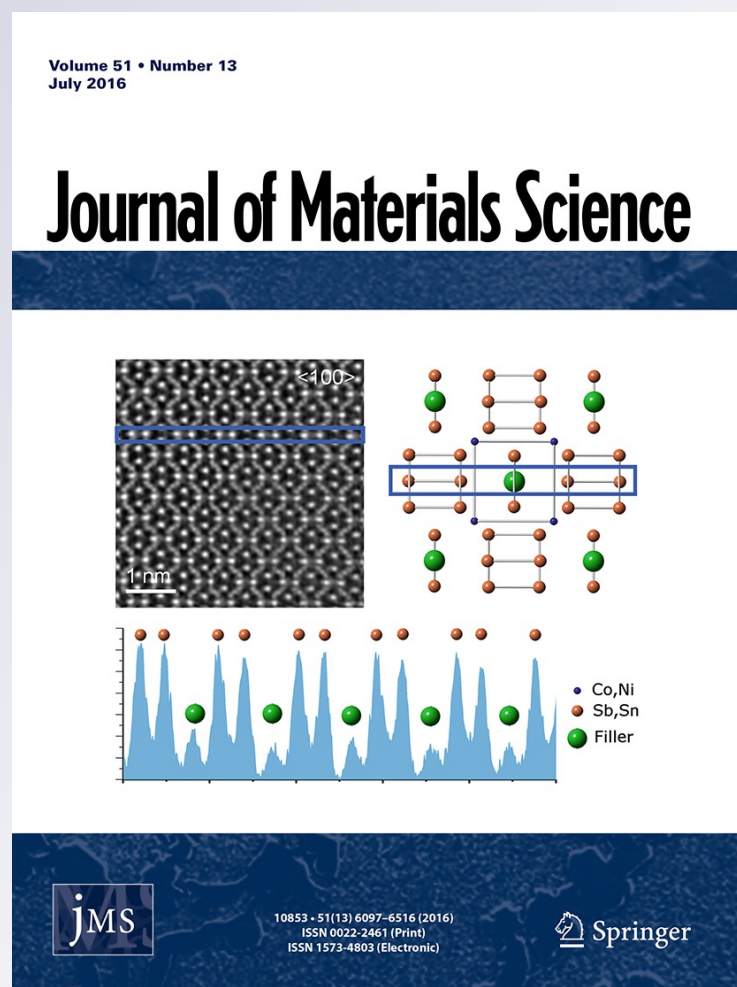
Full Set - Includes 'Journal of Materials Science Letters'

ISSN 0022-2461

Volume 51

Number 13

J Mater Sci (2016) 51:6133-6148
DOI 10.1007/s10853-016-9953-0



Your article is protected by copyright and all rights are held exclusively by Springer Science +Business Media New York. This e-offprint is for personal use only and shall not be self-archived in electronic repositories. If you wish to self-archive your article, please use the accepted manuscript version for posting on your own website. You may further deposit the accepted manuscript version in any repository, provided it is only made publicly available 12 months after official publication or later and provided acknowledgement is given to the original source of publication and a link is inserted to the published article on Springer's website. The link must be accompanied by the following text: "The final publication is available at link.springer.com".



Non-integer temporal exponents in trans-interface diffusion-controlled coarsening

Alan J. Ardell^{1,*}

¹Department of Materials Science and Engineering, Henry Samueli School of Engineering and Applied Science, University of California, Los Angeles, CA 90095-1595, USA

Received: 21 March 2016

Accepted: 2 April 2016

Published online:

11 April 2016

© Springer Science+Business Media New York 2016

ABSTRACT

The kinetics of γ' -type (Ni_3X) precipitate growth and solute depletion in Ni–Al, Ni–Ga, Ni–Ge, Ni–Si, Ni–Ti and Ni–Al–Cr alloys is successfully predicted by the trans-interface diffusion-controlled theory of coarsening using non-integer temporal exponents, n , satisfying $2 \leq n \leq 3$, which are obtained from analyses of particle size distributions (PSDs). The origin of non-integer n is concentration-dependent diffusion through the γ/γ' interface. The literature on diffusion of Al and Ni in Ni_3Al is specifically examined. It is shown unequivocally that the concentration-dependent diffusion of Al can account semi-quantitatively for the value of n that successfully describes the PSDs and kinetics of coarsening of the γ' precipitates. There is no need to invoke a particle size-dependent γ/γ' interface width, as was done in prior work. It is argued that existing theory and computational modeling of coarsening in systems with highly disparate diffusion mobilities in both phases do not correctly represent the mobilities in the matrix, precipitate, and interface in Ni–Al alloys. These theories predict temporal exponents satisfying $3 \leq n \leq 4$, for which there is no experimental support.

Introduction

Late-stage coarsening of precipitates involves the growth of large precipitates at the expense of small ones in a polydisperse assembly embedded in the majority (matrix) phase. When the kinetics of coarsening is controlled by solute diffusion in the matrix phase, the average size, $\langle r \rangle$, of spherical precipitates of radius r increases with time, t , as $\langle r \rangle^3 \approx kt$, where k is a rate constant that includes the physical and thermodynamic parameters of the entire system. As the average particle size increases with t , the average

concentration of solute in the matrix phase, X , decreases approximately as $X \approx (\kappa t)^{-1/3}$, where κ is another rate constant involving the same parameters as k . The iconic theories of Lifshitz and Slyozov [1], and Wagner [2] (the LSW theory) describe this behavior quantitatively and also predict the particle size distribution, PSD, which is independent of t when properly expressed in terms of the variable $u = r/\langle r \rangle$ (scaling behavior). A major premise of the LSW theory is that the matrix phase is a very dilute solid solution and that the particles are highly disperse, so that the LSW theory is valid, strictly

Address correspondence to E-mail: aardell@ucla.edu

speaking, only in the limit $f_e \rightarrow 0$, where f_e is the equilibrium volume fraction of the dispersed phase.

It was recognized quite some time ago, by Lifshitz and Slyozov themselves [1] and, for example, by Asimow [3] and Sarian and Weart [4], that for finite values of f_e , the kinetics of coarsening must increase faster than predicted by LSW. The physical reason for this is straightforward. As f_e increases the average distance separating the particles decreases, the rate of diffusive transport of solute from smaller than average shrinking particles to larger than average growing ones increases. Since the differences in solute concentrations at the particle–matrix interfaces are set by local equilibrium dictated by the Gibbs–Thomson equation, the interface concentrations are independent of f_e . But the fluxes of solute from shrinking to growing precipitates increase as the diffusion distances decrease, which they must do as f_e increases. In a nutshell, this is the origin of the effect of f_e on precipitate coarsening. The rate constants k and κ are no longer dependent solely on the thermo-physical parameters of the system, they also depend on f_e ; symbolically $k = k(f_e)$ and $\kappa = \kappa(f_e)$. The shape of the PSD is also affected by the finite volume fraction, becoming broader as f_e increases.

The diffusive transport of solute in the matrix is very difficult to describe theoretically when f_e is finite, and for this reason it has been modeled in a variety of different ways. The large number of published models make rather different quantitative predictions for the effect of f_e on $k(f_e)$, $\kappa(f_e)$ and the PSDs. These predictions are presented very clearly in the review article by Baldan [5]. Despite disagreements among the various theories, they all have one thing in common: $k(f_e)$ and $\kappa(f_e)$ invariably increase as f_e increases, and the PSDs invariably broaden as f_e increases. A sampling of the predictions of several representative theories [6–10], which is by no means exhaustive, is shown in Fig. 1a. More recent theories of the effect of f_e on coarsening behavior [11–13], published after the review by Baldan, predict dependencies of $k(f_e)/k(0)$ on f_e that lie between the DNS [7] and BW [9] predictions.

The theory of trans-interface diffusion-controlled particle coarsening (TIDC) [14] was stimulated by the complete absence of the expected influence of f_e on the coarsening kinetics of γ' -type precipitates (Ni_3X , with $\text{X} = \text{Al, Ga, Ge, Si, or Ti}$) and their PSDs in five different binary Ni alloys. In other words, the

coarsening behavior of γ' precipitates in these five different binary Ni-X alloys is in utter disagreement with the behavior predicted by the numerous theories (see [5]). In all these alloys, there is actually a slight, unexplained decrease in $k(f_e)$ and $\kappa(f_e)$ when f_e is very small (<0.05), but both rate constants approach a constant value as f_e increases (Ni–Al [15]; Ni–Ga [16]; Ni–Ge [17]; Ni–Si [18–20]; Ni–Ti [21]). To emphasize this point, the dependence of $k(f_e)$ for Ni–Si alloys shown in Fig. 1b; it is representative of the results on the other γ/γ' -type alloys (the only exception is the coarsening behavior of large Ni_3Al precipitates of non-equilibrium shape reported by Lund and Voorhees [22], but there is a ready explanation for this finding in the context of the TIDC theory, as discussed later in “The coarsening of γ' precipitates in Ni-X alloys” section). Such behavior suggests that the traditional view of matrix diffusion-controlled coarsening of γ' precipitates, specifically the LSW theory, and modifications thereof, are incapable of explaining the absence of an effect of f_e on coarsening behavior in Ni-based γ/γ' alloys. It is one thing to produce results that are arguably consistent with the predictions of any particular theory, but quite another to observe behavior that cannot possibly be explained by any of them. It was this conundrum that led to the genesis of the TIDC theory of coarsening in the first place.

We know that γ/γ' interfaces are diffuse in multi-component Ni-based alloys [24–28] as well as in binary Ni–Al alloys where the evidence is experimental [29] and computational [14, 30]. We also know that the diffusion coefficients in Ni_3Al are between one and two orders of magnitude smaller than in Ni–Al solid solutions at temperatures of typical coarsening experiments (800–1000 K) [31–34]. In order for γ' precipitates to grow or shrink, solute must be transported through the γ/γ' interface. Since diffusion through the ordered region of the interface is the slower step, it is by necessity the rate-controlling one. Implicitly, coarsening behavior under conditions of trans-interface diffusion control must be completely independent of f_e . Assuming that the width of the interface, δ , is independent of r , and that all the other thermo-kinetic parameters that govern transport through the interface are also independent of r , the TIDC [14] theory predicts a temporal exponent, n , equal to 2, i.e., $\langle r \rangle^2 \approx k_T t$ and $X \approx (\kappa_T t)^{-1/2}$ at very long aging times; k_T and κ_T are the TIDC counterparts of k and κ in the LSW theory and both are completely

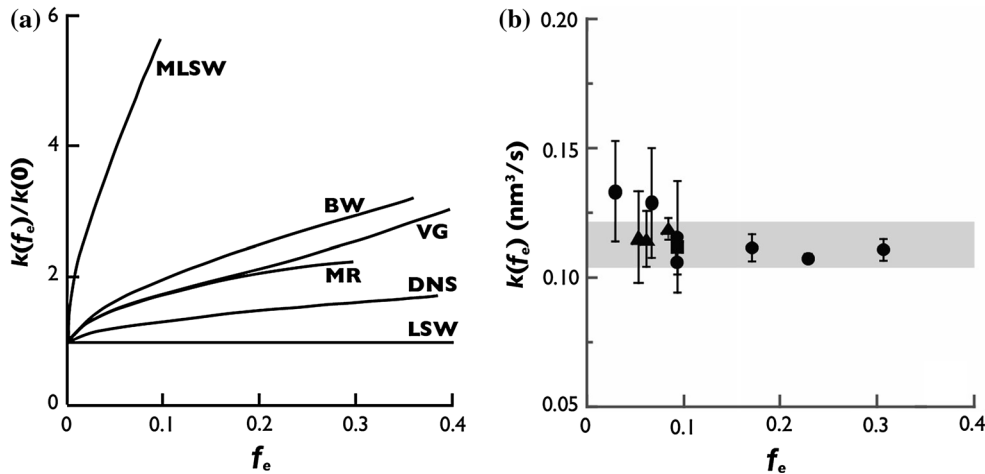


Figure 1 **a** The dependencies of the rate constant for particle growth during coarsening, $k(f_e)$, normalized by the rate constant of the LSW theory, $k(0)$, predicted by 5 theories: MLSW [6], DNS [7], MR [8], BW [9], and VG [10]. **b** The experimentally measured values of $k(f_e)$ for the coarsening of γ' Ni₃Si precipitates in

different Ni–Si alloys aged at 650 °C. The plotting symbols in (b) refer to the data of *filled triangle* Meshkinpour and Ardell [18], *filled circle* Cho and Ardell [20], and *filled square* Sauthoff and Kahlweit [23]. The shaded area in (b) contains the majority of the data on $k(f_e)$.

independent of f_e . Under these conditions, the PSD becomes broader than the LSW result and is in fact equivalent to the PSD derived by Wagner [2] for the case of interface reaction-controlled coarsening; the temporal exponent for that mode of coarsening is also $n = 2$.
Ardell and Ozolins [14] briefly considered the possibility that δ might actually vary with r , arguing that precipitates approaching the dimensions of several unit cells of the L1₂ structure would lose their identity as a distinct phase unless the interface sharpened for very small values of r . In subsequent papers [35–39], this conjecture was made quantitative by assuming a relationship of the form $\delta \propto r^m$, with m satisfying $0 \leq m \leq 1$, ultimately leading to a temporal exponent of $n = m + 2$. According to the TIDC theory for arbitrary values of m , the kinetics of particle growth and solute depletion in a binary alloy system obeys the equation

$$\frac{d\langle r \rangle^n}{dt} = k_T, \tag{1}$$

integration of which produces the equation for the growth of the average precipitate, namely

$$\langle r \rangle^n - \langle r_0 \rangle^n = k_T t, \tag{2}$$

where $\langle r_0 \rangle$ is the average radius at the onset of coarsening. As the average precipitate grows, the concentration of solute in the matrix decreases with t according to the equation

$$X - X_e \approx (\kappa_T t)^{-1/n}, \tag{3}$$

where X_e is the concentration of solute at thermodynamic equilibrium. The PSDs are also dependent upon n and are given by the equations [35–37]¹

$$h(z) = -3f(z) \exp\{3p(z)\} \tag{4}$$

where $p(z)$ is the function

$$p(z) = \int_0^z f(x) dx \tag{5}$$

and $f(z)$ is the function

$$f(z) = \frac{[z(n-1)]^{(n-1)}}{n^n(z-1) - z^n(n-1)^{(n-1)}}. \tag{6}$$

In Eqs. (4)–(6) $z = r/r^*$; see Eq. (7) for the definition of r^* . For comparison with experimentally determined PSDs, it is necessary to use the function $g(u)$, where $u = r/\langle r \rangle$ and $g(u) = \langle u \rangle h(z)$. The maximum allowable scaled particle size in the distribution, u_{max} , is $n/(n-1)$.

A particularly attractive feature of this aspect of the TIDC theory is that the dependence of the PSDs on n quantitatively connects the PSDs with the kinetics. Analysis of previously published experimental data on the γ' PSDs Ni–Al, Ni–Ga, Ni–Ge, Ni–Si, and Ni–Ti alloys [37] confirms the efficacy of the TIDC

¹ The factor of 3 in the exponential term in Eq. (4) was mistakenly omitted in [35–37], but was included in all fitting of experimental PSDs.

theory, via fitting the PSDs to determine the “best” value of n and then analyzing the data on kinetics using this particular non-integer value of n to extract values of the interfacial free energy, σ , from the experimentally measured rate constants k_T and κ_T . It is not an overstatement to claim that the TIDC theory is the only published theory to date that successfully couples the parameter that governs the shape of the PSD with the kinetics of growth of the average particle and the kinetics of solute depletion. Moreover, the extension of the theory to describe the kinetics of coarsening of precipitates in ternary alloys [38] is similarly successful in describing the coarsening behavior of γ' precipitates in ternary Ni–Al–Cr alloys [39].

An additional issue related to TIDC coarsening is worth emphasizing. Imagine reversing the matrix and precipitate phases in these same Ni-based alloys! Diffusion in the ordered matrix phase is now slower than diffusion through the interface, so matrix diffusion becomes rate controlling, and the conditions for LSW-type coarsening behavior should prevail. Under these conditions, the kinetics of particle growth should obey $\langle r \rangle^3 \approx k(f_e)t$, and there should be a palpable effect of f_e on $k(f_e)$. This is in fact exactly what happens for the coarsening of γ (Ni–X solid solution) precipitates in two so-called “inverse” Ni₃Al and Ni₃Ge alloys. As seen in Fig. 2, the rate constants $k(f_e)$ increase dramatically with f_e over the ranges studied. These ranges are necessarily restricted due to the compositions of the phase boundaries in Ni₃Al/Ni–Al and Ni₃Ge/Ni–Ge alloys, so it is not possible to explore the vast range of f_e accessible in normal binary alloys, similar to the data shown in Fig. 1b. It is nevertheless quite evident in Fig. 2 that

the dependencies of $k(f_e)$ for the coarsening of γ precipitates in inverse Ni₃Al and Ni₃Ge alloys are very strong.

From a purely physical perspective, the observations on the effect of f_e on the coarsening behavior of γ' precipitates in normal Ni–X alloys and γ precipitates in inverse Ni₃Al and Ni₃Ge alloys are satisfactorily explained. There is no other way to rationalize the observed behavior other than by accepting the predominant role that long-range order plays in the diffusive transport of solute atoms through the γ/γ' interface in these alloys. From a quantitative, predictive point of view, however, the theoretical rationale for coupling the temporal exponent and the PSDs has been predicated solely on the assumption that δ slowly increases as r increases. Until recently, the measurements of Booth-Morrison et al. [43] on the Al concentration profiles across γ/γ' interfaces in a ternary Ni–Al–Cr alloy provided the sole support for this assertion. In their work, the complete concentration profiles are difficult to measure for the smaller particle sizes, but it is evident in their Fig. 4 that the gradient across the interface decreases with the increasing particle size (or aging time), suggesting that δ increases as the size increases. This assertion was further supported by modeling the interfaces using the sigmoid function to represent the concentration profile [44].

That situation has changed to a large extent with the results of several investigations in which measurements of δ with t have been reported [28, 29, 45]. Plotnikov et al. [29] published data showing that δ for the Ni–Al/Ni₃Al interface decreases rapidly at small particle sizes, the order of the interface width, and continues to decrease slightly during the coarsening

Figure 2 Data on the rate constants for coarsening, $k(f_e)$, of γ (Ni–Al or Ni–Ge) precipitates in “inverse” a Ni₃Al [40] and b Ni₃Ge [41] alloys. The curves in both the figures are predictions of the MSLW theory [6] modified by the calculations of Tsumuraya and Miyata [42].

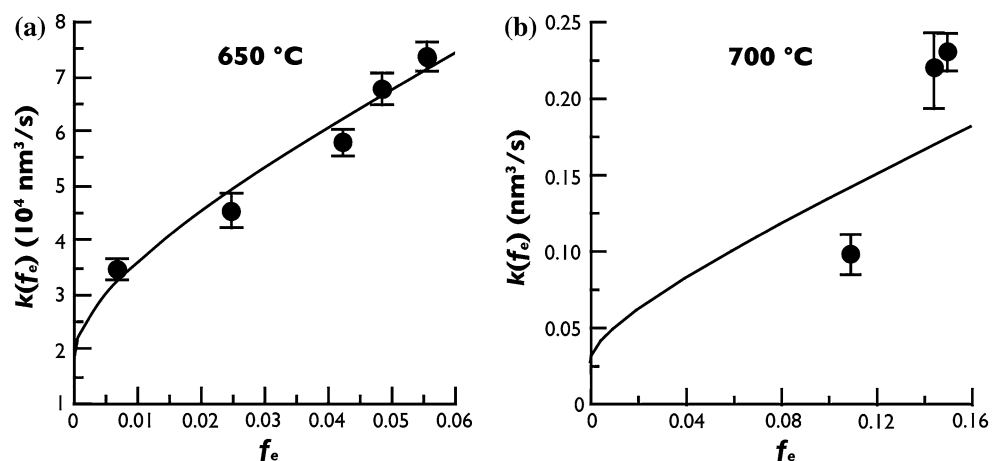
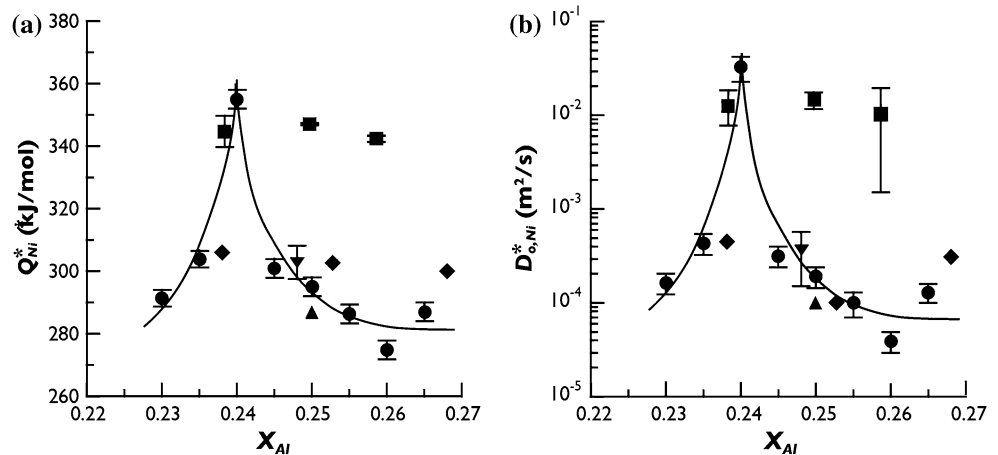


Figure 3 The dependencies of the activation energies, Q_{Ni}^* , and pre-exponential factors, $D_{0,Ni}^*$, on the concentration of Al, X_{Al} , in Ni_3Al for the tracer diffusion coefficients of Ni in Ni_3Al . Data of filled diamond Hancock [65], filled triangle Bronfin et al. [66], filled square Hoshino et al. [67], filled downward triangle Frank et al. [68] and filled circle Shi et al. [69].



regime. Meher et al. [28] reported somewhat similar results for the γ/γ' interface in ternary Ni–Al–Cr alloys, but in their alloy δ is essentially constant during late-stage coarsening. Al-Kassab et al. [45] reported that the width of the Ni–Ti/ Ni_3Ti interface is essentially constant for 2 aging times in the coarsening regime. These observations that δ is approximately constant during coarsening suggest that the temporal exponent for TIDC coarsening should be $n = 2$ for γ' coarsening in all three alloys, and by implication in all the others as well. Furthermore, a constant interface width during coarsening potentially obviates any physical argument for non-integer values of n .

There is no doubt that the temporal exponent that best fits the PSDs for γ' precipitate coarsening in Ni–Al alloys is $n = 2.4$ [36], and there is no doubt that non-integer values of n best fit the PSDs for γ' coarsening in the other binary Ni-based alloys as well. Absent a concentration-dependent interface width, this can be explained by the TIDC theory only if some other factor is incorporated into the theory to account for non-integer values of n , in particular a factor that depends relatively strongly on alloy concentration over the small concentration changes attendant to particle coarsening. The most obvious candidate is the intrinsic diffusion coefficient of Al in Ni_3Al , which is already quite well known to be

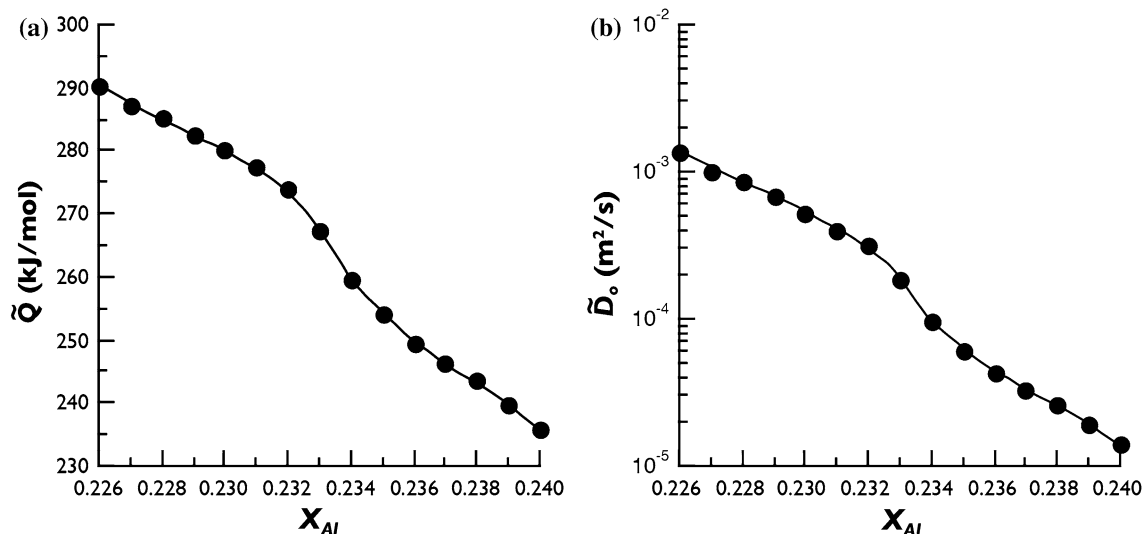


Figure 4 The dependencies on composition, X_{Al} , in Ni_3Al of the activation energy, \tilde{Q} , (a) and pre-exponential factor, \tilde{D}_0 , (b) for chemical diffusion in Ni_3Al ; Data of Fujiwara and Horita [32].

concentration dependent (see Campbell [46] for a compendium of results).

In this context, it should be noted that concentration-dependent atomic mobilities have been incorporated into theories of late-stage spinodal decomposition (well into the coarsening regime) [47–53], and that phase field simulations of γ' precipitate coarsening have used similar assumptions [54, 55]. These works show that with suitably chosen functions for the mobility of solute, particularly functions that represent extremely slow diffusion in the precipitate phase, the temporal exponent n actually increases from 3 to as much as 4, with the irony that the kinetics in these papers is attributed to interface diffusion control. Obviously, these predictions are entirely contrary to those of the TIDC theory, and for the most part, they are completely unsupported by experimental evidence. The only theories of coarsening derived using the methodology of LSW, taking diffusion-dependent diffusivity into account, are those of Che and Hoyt for zero [56] and finite [57] volume fractions. They found no effect on the temporal exponent during late-stage coarsening, but they do predict important effects during transient ripening, especially for finite volume fractions; these considerations do not apply here.

The main purpose of the work reported in this paper is to explore the possibility that concentration-dependent diffusion in Ni_3Al can affect the kinetics of coarsening and yield non-integer temporal exponents in the range $2 \leq n \leq 3$. We will see that this is indeed the case. The theories and simulations which predict values of $n > 3$ as manifestations of interface diffusion control will be discussed.

The role of concentration-dependent diffusion in Ni_3Al

In the TIDC theory [14], the growth rate, dr/dt , of a particle of radius r is

$$\frac{dr}{dt} = \frac{2\sigma V_m D_{\text{IAI}}}{\delta(\Delta X_{\text{eAl}}^{\gamma/\gamma'}) G''_{\text{m}\gamma}} \left(\frac{1}{r^*} - \frac{1}{r} \right), \quad (7)$$

where σ is the interfacial free energy of the γ/γ' interface, V_m is the molar volume of the γ' phase, D_{IAI} is the coefficient of diffusion of Al in the interface, $\Delta X_{\text{eAl}}^{\gamma/\gamma'}$ is the difference between the Al concentrations

in the γ and γ' phases at thermodynamic equilibrium ($\Delta X_{\text{eAl}}^{\gamma/\gamma'} = X_{\text{eAl}}^{\gamma'} - X_{\text{eAl}}^{\gamma}$), $G''_{\text{m}\gamma}$ is the curvature of the molar Gibbs free energy of mixing of the γ phase, evaluated at $X_{\text{eAl}}^{\gamma'}$, and r^* is the radius of the critical particle which is momentarily in (unstable) equilibrium with the ensemble of particles and is neither growing nor shrinking at time t . Equation (7) is written explicitly for a two-phase binary γ/γ' alloy but is easily generalized for a system with matrix α and precipitate β phases. The extension to ternary alloys is a bit more complicated but has been dealt with theoretically in the literature [38, 58–61]. Keep in mind that r^* is not necessarily equal to the average radius $\langle r \rangle$. It happens that $r^* = \langle r \rangle$ in the LSW theory, but in other kinds of coarsening processes, including TIDC coarsening, these two parameters are not equal. The relationship between r^* and $\langle r \rangle$ is simply $\langle r \rangle = \langle u \rangle r^*$, where $\langle u \rangle \leq 1$ is obtained from the PSD.

When δ is constant, n can never be >2 unless another parameter in Eq. (1) varies appropriately with r . The most obvious choice is D_{IAI} , which represents the intrinsic diffusion coefficient of Al in the diffuse γ/γ' interface. In the TIDC theory, D_{IAI} is a weighted average interfacial diffusion coefficient, varying between its relatively high value in the matrix and relatively low value in the ordered γ' phase. In reality, D_{IAI} is expected to be closer in value to the intrinsic diffusivity of Al in the γ' phase.

The dependence of D_{IAI} on r comes about in the following way. We already know that diffusion of Al in ordered Ni_3Al is composition dependent at high temperatures, e.g., 1400 K, from the data of Numakura et al. [62], and increases with increasing Al concentration. For the analysis of data on coarsening, data on the diffusion of Al in Ni_3Al are needed at low temperatures, specifically 898 and 988 K [36, 63]. There are no direct measurements of tracer diffusion of Al in Ni_3Al due to the absence of a suitable Al isotope. To obtain such data, it is therefore necessary to evaluate data on the tracer diffusion of Ni in Ni_3Al , D_{Ni}^* , and the chemical diffusion coefficient in Ni_3Al , \tilde{D} , and use the relationship

$$\tilde{D} = (X_{\text{Al}} D_{\text{Ni}}^* + X_{\text{Ni}} D_{\text{Al}}^*) \Phi = X_{\text{Al}} D_{\text{Ni}} + (1 - X_{\text{Al}}) D_{\text{Al}}, \quad (8)$$

where D_{Ni} and D_{Al} are the intrinsic diffusion coefficients of Ni and Al in Ni_3Al , Φ is the thermodynamic factor, defined by

$$\Phi = X_{Al} \frac{d \ln a_{Al}}{d X_{Al}} = \frac{d \ln a_{Al}}{d \ln X_{Al}}, \quad (9)$$

a_{Al} is the activity of Al in Ni_3Al , S is the vacancy wind factor [64], and the superscript γ' on X_{eAl} has been dropped as no longer needed. Fortunately, D_{Ni}^* , \tilde{D} , and a_{Al} have all been measured at high temperatures (1400–1600 K). Estimates of these parameters at the lower temperatures of the experiments on coarsening involve extrapolations over a large range of T , but there is no other option. D_{Al} is taken as the diffusion coefficient approximately equal to D_{IAI} .

We first consider the measurements of D_{Ni}^* reported in several investigations [65–69]. The activation energies and pre-exponential factors for tracer diffusion in Ni_3Al , Q_{Ni}^* , and $D_{0,Ni}^*$, respectively, are shown as functions of composition in Fig. 3. With the exception of 2 data points from the work of Hoshino et al. [67], both quantities pass through a sharp maximum at around $X_{Al} = 0.24$. The maxima in Q_{Ni}^* and $D_{0,Ni}^*$ have been discussed by Shi et al. [69], but there is no convincing argument for their existence. Whatever the reason, there is little doubt that both quantities decrease from their maxima for $X_{Al} < 0.24$. Chemical diffusion in Ni_3Al has been measured as a function of composition by Fujiwara and Horita [32], the activation energies, and pre-exponential factors for which \tilde{Q} and \tilde{D}_0 , respectively, computed from the results shown in their Fig. 3, are shown in Fig. 4. Both quantities decrease with the increasing X_{Al} .

To proceed, we need to estimate the activity of Al in Ni_3Al as a function of composition, and to this end select the data of Hilpert et al. [70]. Their data, organized by Ikeda et al. [71] is reproduced in Fig. 5a, where it is seen that the relationship between $\log a_{Al}$ and X_{Al} is linear to a good approximation at 1400, 1500 and 1600 K. The temperature dependencies of a_{Al} are of the Arrhenius type at any given composition [71], and hence, the activities of Al in Ni_3Al at 898 and 988 K can be evaluated from Arrhenius plots to extrapolate the activities to the lower temperatures relevant to this work. This is done for $X_{Al} = 0.23, 0.24$ and 0.25 , leading to the results shown in Fig. 5b. Assuming that the relationship between $\log a_{Al}$ and X_{Al} at 898 and 988 K is linear at low temperatures, as it appears to be at high temperatures (Fig. 5a), all the input needed to calculate D_{Al} as a function of composition at these two temperatures becomes available.

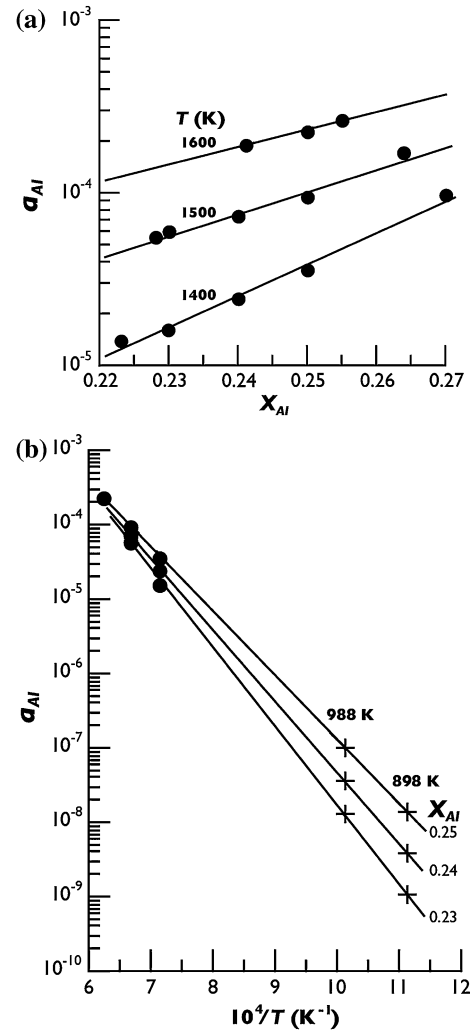


Figure 5 **a** Plots of the activity of Al, a_{Al} , versus concentration, X_{Al} , in Ni_3Al at the 3 temperatures indicated, taken from the work of Hilpert et al. [70] and Ikeda et al. [71]; **b** Arrhenius plots of a_{Al} , for $X_{Al} = 0.23, 0.24$, and 0.25 . The activities of Al as functions of composition are indicated by + symbols.

The calculations of D_{Al} are done for four compositions, using the data of Hoshino et al. [67] ($X_{Al} = 0.2384$) and the data of Shi et al. [69] ($X_{Al} = 0.230, 0.235$, and 0.240) on Q_{Ni}^* and $D_{0,Ni}^*$ in Fig. 3 to first calculate D_{Ni}^* . The intrinsic diffusivities of Ni in Ni_3Al , D_{Ni} , are then readily calculated using the relationship $D_{Ni} = \Phi D_{Ni}^*$ (assuming for now that $S = 1$), using Eq. (6) to calculate Φ from the linear equations relating $\log a_{Al}$ and X_{Al} at 898 and 988 K. The chemical diffusion coefficients at these temperatures are then estimated from the values of \tilde{Q} and \tilde{D}_0 shown in Fig. 4, and, finally, D_{Al} is calculated using

Eq. (8). The values of all the parameters are shown in Tables 1, 2 for the two aging temperatures of interest.

The magnitude of S is difficult to determine over the full range of compositions and temperatures relevant to these estimates, but it is possible to estimate its importance using the tracer diffusivities of Al [72] and Ni [73] and the calculations of Belova and Murch [74], who report values of S as functions of the ratios D_{Al}^*/D_{Ni}^* and D_{Ni}^*/D_{Al}^* . At 898 and 988 K, the relevant ratios D_{Ni}^*/D_{Al}^* are 0.51 and 0.91. For $X_{Al} = 0.23$, $S \approx 1$, justifying the assumption used in the calculations.

To see how well this conjecture works, the data on D_{Al} and in Tables 1, 2 are plotted in Fig. 6 as $\log D_{Al}$ versus $\log (X_{Al} - X_{eAl})$, presupposing that $D_{IAI} \approx D_{Al}$ a relationship of the type

$$D_{Al} \approx \hat{D}(X_{Al} - X_{eAl})^m, \tag{10}$$

where m satisfies the condition $0 < m < 1$ and \hat{D} is a constant. The concentration differences are estimated using the equilibrium values of X_{eAl} at the two aging temperatures ($X_{eAl} = 0.22948$ at 898 K and 0.22689 at 988 K), calculated using the equilibrium γ solvus curve of Ma and Ardell [75]. It is evident in Fig. 6 that the relationships are not linear, but it is also quite apparent that the slopes of the curves diminish to values smaller than unity as X_{Al} approaches X_{eAl} . If the data are fitted to a parabola, the slopes at the smallest values of X_{Al} ($=0.23$) are approximately 0.9 and 0.3 at 898 and 998 K, respectively; the dashed line shown in the figure has a slope $m = 0.4$. Strictly speaking, Eq. (10) cannot be correct in the limit

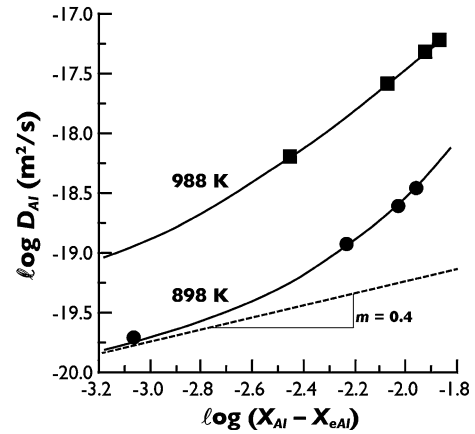


Figure 6 Plots of the logarithm of the intrinsic diffusion coefficient of Al in Ni_3Al , D_{Al} , versus the logarithm of the difference between the concentrations of Al in hypostoichiometric Ni_3Al , X_{Al} , and the concentration in equilibrium with the γ (Ni–Al) solid solution, X_{eAl} , at 2 temperatures of interest. The curves shown are not fitted to the data, but serve as a guide to the eye. The dashed line has a slope, $m = 0.4$, which leads to the temporal exponent $n = 2.4$ used in [36].

$X_{Al} = X_{eAl}$, because D_{Al} approaches zero, which is clearly an impossible result. However, it takes a very long time during coarsening to reach thermodynamic equilibrium, and hence, Eq. (10) is a realistic approximation under typical experimental conditions, where $X_{Al} - X_{eAl}$ is the order of 10^{-4} . Considering that the complexity of trans-interface diffusion in a polydisperse assembly of precipitates is difficult to capture in a single equation, the utility of Eq. (10) is rationalized due to its simple form and ready

Table 1 Values of the parameters used in the calculations of D_{Al} at 898 K in conjunction with $X_{eAl} = 0.22948$

X_{Al}	D_{Ni}^* (m ² /s)	Φ	D_{Ni} (m ² /s)	\tilde{Q} (kJ/mol)	\tilde{D}_0 (m ² /s)	\tilde{D} (m ² /s)	D_{Al} (m ² /s)
0.2300	1.795×10^{-21}	28.941	5.196×10^{-20}	280.021	5.307×10^{-4}	2.730×10^{-20}	1.993×10^{-20}
0.2350	8.992×10^{-22}	29.570	2.659×10^{-20}	254.255	6.196×10^{-5}	1.005×10^{-19}	1.232×10^{-19}
0.2384	1.163×10^{-22}	29.998	3.490×10^{-21}	242.205	2.376×10^{-5}	1.936×10^{-19}	2.531×10^{-19}
0.2400	7.115×10^{-23}	30.199	2.149×10^{-21}	236.015	1.427×10^{-5}	2.664×10^{-19}	3.499×10^{-19}

Table 2 Values of the parameters used in the calculations of D_{Al} at 988 K in conjunction with $X_{eAl} = 0.22689$

X_{Al}	D_{Ni}^* (m ² /s)	Φ	D_{Ni} (m ² /s)	\tilde{Q} (kJ/mol)	\tilde{D}_0 (m ² /s)	\tilde{D} (m ² /s)	D_{Al} (m ² /s)
0.2300	6.283×10^{-20}	24.001	1.508×10^{-18}	280.021	5.307×10^{-4}	8.316×10^{-19}	6.296×10^{-19}
0.2350	3.667×10^{-20}	24.523	8.993×10^{-19}	254.255	6.196×10^{-5}	2.235×10^{-18}	2.646×10^{-18}
0.2384	7.808×10^{-21}	24.502	1.913×10^{-19}	242.205	2.376×10^{-5}	3.718×10^{-18}	4.822×10^{-18}
0.2400	5.416×10^{-21}	25.045	1.356×10^{-19}	236.015	1.427×10^{-5}	4.744×10^{-18}	6.200×10^{-18}

adaptability to the equations of coarsening. A temporal exponent of 2.4, relevant to γ' coarsening in Ni–Al alloys, emerges naturally from the condition $n = m + 2$.

The temporal exponent for coarsening is formally manifested through the Gibbs–Thomson equation for the precipitate phase, which has the same form as it does for the matrix phase, i.e.,

$$X_{Al} - X_{eAl} = \frac{\ell_{\gamma'}}{r}, \tag{11}$$

where $\ell_{\gamma'}$ is the capillary length for the γ' phase, which is given by the equation [76]

$$\ell_{\gamma'} = \frac{2\left\{\bar{V}_{Ni}^{\gamma'}(1 - X_{Al}^{\gamma'}) + \bar{V}_{Al}^{\gamma'}X_{Al}^{\gamma'}\right\}\sigma}{\Delta X_{eAl}^{\gamma/\gamma'} G_{m\gamma'}''} = \frac{2\bar{V}_m}{\Delta X_{eAl}^{\gamma/\gamma'} G_{m\gamma'}''}, \tag{12}$$

where $\bar{V}_{Ni}^{\gamma'}$ and $\bar{V}_{Al}^{\gamma'}$ are the partial molar volumes of Ni and Al in the γ' phase, $G_{m\gamma'}''$ is the curvature of the Gibbs free energy of mixing of the γ' phase, evaluated at $X_e^{\gamma'} = X_{eAl}^{\gamma'}$. On first substituting Eq. (12) into (11) and then (10) and ultimately into Eq. (7), the expression for the growth rate of an individual particle of radius r becomes

$$\frac{dr}{dt} = \frac{2\sigma V_m \hat{D}}{\delta(\Delta X_{eAl}^{\gamma/\gamma'})^2 G_{m\gamma'}''} \left\{ \frac{2\sigma \bar{V}_m}{\Delta X_{eAl}^{\gamma/\gamma'} G_{m\gamma'}''} \right\}^m \frac{1}{r^m} \left(\frac{1}{r^*} - \frac{1}{r} \right) \tag{13}$$

Following established procedures [14, 36] to generate the equations describing the variations of $\langle r \rangle$ and X_{Al} with aging time, we arrive at Eqs. (2) and (3), with the rate constants k_T and κ_T expressed as

$$k_T = \left\{ \frac{2(n-1)\sigma}{n} \right\}^{(n-1)} \left[\frac{\langle u \rangle^n V_m \bar{V}_m^{n-2} \hat{D}}{\delta(\Delta X_{eAl}^{\gamma/\gamma'})^n G_{m\gamma'}'' (G_{m\gamma'}'')^{(n-2)}} \right] \tag{14}$$

and

$$\kappa_T = \left\{ \frac{(n-1)G_{m\gamma'}''}{nV_m} \right\}^{(n-1)} \left[\frac{\bar{V}_m}{G_{m\gamma'}''} \right]^{(n-2)} \frac{\hat{D}}{2\delta\sigma} \tag{15}$$

On dividing Eq. (11) by (12) and solving for σ , we obtain the result

$$\sigma = \frac{G_{m\gamma'}'' \Delta X_{eAl}^{\gamma/\gamma'}}{2\langle u \rangle V_m} \left(\frac{k_T}{\kappa_T} \right)^{1/n}, \tag{16}$$

which is exactly the same equation derived previously [36] assuming that δ rather than D_{IAl} depends on r . In other words, treating diffusion as is done herein has no impact at all on the values of σ

extracted from data on coarsening. It also has no impact whatsoever on the PSDs, which are governed by Eqs. (4) to (6) [35, 36].

Discussion

The coarsening of γ' precipitates in Ni-X alloys

The results and analyses presented in “The role of concentration-dependent diffusion in Ni₃Al” section demonstrate convincingly that a non-integer temporal exponent, n , satisfying the condition $2 \leq n \leq 3$ arises naturally from the concentration dependence of diffusion in Ni₃Al. There is therefore no need to invoke a size-dependent interface width to account for the non-integer value of $n = 2.4$ previously reported for this alloy. Although not as extensively investigated, the aforementioned absence of an effect of f_e on coarsening behavior in Ni–Ga, Ni–Ge, Ni–Si, and Ni–Ti alloys, and for that matter in ternary Ni–Al–Cr alloys, naturally leads to the expectation that the explanation for this finding is identical in those alloy systems.

Of the 5 binary Ni-X alloys, diffusion in the Ni₃X phases has been measured as a function of solute concentration only in Ni₃Ga and Ni₃Ge. The L1₂ crystal structure of Ni₃Ti is metastable, so diffusion in it cannot be measured. The L1₂ crystal structure of Ni₃Si is stable only below ~ 1130 °C [77], thereby rendering measurement of diffusion of Si in Ni₃Si by conventional methods very difficult; no such measurements exist. There have been measurements of diffusion as a function of concentration in ternary Ni₃(Al,Cr) alloys, but there are not enough data to extrapolate to the low temperatures and γ' concentrations in the coarsening regimes. Of the Ni₃Ga and Ni₃Ge phases, there is convincing evidence that both chemical and intrinsic diffusion of Ga in Ni₃Ga increases with increasing solute concentration at low temperatures [78–80], therefore mimicking the behavior of diffusion in Ni₃Al. The data on the diffusion of Ge in Ni₃Ge are more limited. Komai et al. [81] report that \tilde{D} in Ni₃Ge increases rapidly with increasing Ge content at temperatures below ~ 970 °C, and Numakura et al. [62] report similar behavior at ~ 920 °C. However, the tracer diffusion coefficient, D_{Ge}^* , decreases with the increasing Ge concentration at $T > 920$ °C. Unfortunately, the

concentration dependence of the intrinsic Ge diffusion coefficient cannot be predicted without knowledge of the thermodynamic factor, which has not been determined for Ni₃Ge. The very strong concentration dependence of \tilde{D} suggests that the intrinsic diffusivities of both components ($D_{\text{Ni}} = D_{\text{Ni}}^* \Phi S$ and $D_{\text{Ge}} = D_{\text{Ge}}^* \Phi S$) should increase similarly through the concentration dependence of Φ . It therefore seems safe to conclude that the coarsening of γ' -type precipitates in binary Ni-X alloys is controlled by diffusion through the γ/γ' interface, with temporal exponents satisfying $n < 3$, and with no effect of volume fraction and no need to invoke precipitate size-dependent interface widths to account for the kinetics or predicting the PSDs.

Turning now to the volume fraction dependence of γ' coarsening measured by Lund and Voorhees [22], it is important to contextualize the circumstances involved in their measurements. They investigated very late-stage coarsening of large γ' particles that were far from their equilibrium shapes; elastic interactions had already intervened to produce primarily plate-shaped or lath-shaped particles. They did not measure $\langle r \rangle$ as a function of t but instead measured surface area per unit volume as the most convenient and accessible metric of particle size. Measuring PSDs under these circumstances is out of the question. Ardell and Ozolins [14] pointed out that when the condition $r \gg \delta D_{\text{Al}}^\gamma / D_{\text{IAl}}$, where D_{Al}^γ is the coefficient of solute diffusion in the matrix phase, the coarsening behavior becomes matrix diffusion controlled. The physical reason for this is that when the particles are very large, the concentration gradients in the matrix become so small that diffusion of solute in the matrix is actually slower than it is through the interface. An estimate of the particle radius at the transition from trans-interface to matrix diffusion control, r_T , is simply $r_T \approx \delta D_{\text{Al}}^\gamma / D_{\text{IAl}}$. Taking $\delta = 2$ nm and $D_{\text{Al}}^\gamma / D_{\text{IAl}} = 0.05$ as representative values, $r_T \approx 100$ nm. This might seem like a small particle size, but it is nearly an order of magnitude larger than the largest non-agglomerated average particle radius reported by Ardell and Nicholson [82] ($\langle r \rangle = 17.3$ nm). From their published figures, it is easy to see that the average “diameters” of the γ' precipitates measured by Lund and Voorhees [22] are between 0.5 and 1 μm , which is far in excess of r_T . This provides clear rationalization for the assertion that there is no contradiction between the results of

Lund and Voorhees and the predictions of the TIDC theory.

Relationship to coarsening in systems with highly disparate diffusion mobilities

We consider here the connections between the results in this work on coarsening and diffusion in γ/γ' alloys and theories and computational simulations that predict temporal exponents >3 . Langer et al. [47] suggested that a concentration-dependent mobility, $M(X) = K(1-X^2)$, satisfies the conditions specified by Cahn and Hilliard for describing the free energy of a compositionally non-uniform system [83]; K is a temperature-dependent constant. Langer et al. did not pursue this suggestion mathematically but noted that the kinetics in late stages of spinodal decomposition could be seriously impacted at concentrations approaching $X \approx 1$. Kitahara and Imada [53] and Kitahara et al. [48], using a similar expression for the mobility, $M = K(1-\beta X)$, where β is a constant, showed that if $\beta X \approx 1$, diffusion in the minority phase during late-stage coarsening becomes very slow and that the temporal exponent becomes $n = 4$. They allege that interface diffusion dominates the kinetics. The computer simulations of Lacasta et al. [52] further explored the influence of β on the temporal exponent and showed that in the late stages of coarsening, n can actually approach ~ 4.5 as β approaches unity. Bray and Emmott [50] explored the effect of a mobility satisfying the equation $M(X) = K(1-X^2)^\alpha$, where α is an exponent satisfying the condition $\alpha \geq 1$, and showed theoretically that the temporal exponent becomes $n = 3 + \alpha$ during late-stage coarsening. It should be noted that all these theories utilize a “double-well” free energy function of the form $G(X) \propto (1-X^2)^2$, with minima at $X = \pm 1$.

Sheng et al. [54] explored the impact of several different concentration-dependent mobilities, including those mentioned above, and concluded that temporal exponents of $n \approx 3.35$ are characteristic of late-stage coarsening whenever the mobility in the precipitate phase is much smaller than that in the matrix phase, actually approaching zero. They cited the data reported in Fig. 1 of a paper by Seidman et al. [84] as experimental evidence supporting the results of their computer simulations, using the knowledge that diffusion in the ordered γ' precipitates in a ternary Ni–5.2Al–14.2Cr (at.%) alloy is much slower than in the matrix. Similar to their

predecessors, Sheng et al. [54] attributed their findings to interface diffusion-controlled coarsening. Inspired by the simulations of Sheng et al., Dai and Du [85] mathematically examined the implications of a dimensionless mobility $M^* = 1 + u$, where u is a dimensionless concentration that satisfies $-1 \leq u \leq 1$, so that for $u \approx -1$ in the precipitate phase $M^* \rightarrow 0$. They did not report the temporal exponent for this model but affirmed the findings of Sheng et al. Dai and Du [55] subsequently performed detailed mathematical and computational studies of the impact of three different dimensionless mobility expressions, $M^* = 1$, $M^* = |1 - u^2|$ and $M^* = |1 + u|/2$, on late-stage coarsening behavior. Constant mobility, $M^* = 1$, always produces a temporal exponent $n = 3$, but for $M^* = |1 - u^2|$, the temporal exponent is $n = 4$ for late-stage coarsening. They suggested that a temporal exponent between 3 and 4 might be a consequence of transient ripening behavior.

These theoretical and computational findings beg the question of the relevance of the TIDC theory. To be clear, the phase diagrams in the alloy systems investigated computationally all have miscibility gaps. The diffusional mobilities of the components are treated as highly disparate using the types of functions mentioned above. Initial phase separation occurs by spinodal decomposition, tracked by solution of the Cahn–Hilliard equation in 2 dimensions, and allowed run for long times until the late stages are reached at which time coarsening is the dominant mode of particle growth. The kinetics in these simulations is inevitably governed by an equation with the form of Eq. (2), but with $n > 3$ and sometimes exceeding 4. It is obvious that there is no conceivable compatibility between these simulations and the TIDC theory. The connection between slow diffusion in the precipitate phase and interface diffusion control espoused by the works of these authors [48–50, 52, 53, 55, 85] further compromises the TIDC theory. To make sense of the basic tenets of the TIDC theory in the face of these findings, we need to look more closely at the general framework of phase transformations, diffusion and thermodynamics, as physical, rather than mathematical and computational, concepts.

Consider first diffusion in the real Ni–Al alloy system. In this regard most of the work has already been done in “The role of concentration-dependent diffusion in Ni_3Al ” section. The general equations of coarsening in the absence of spinodal decomposition

in particular, and unstable solid solutions in general, involve solutions to Fick’s laws using diffusion coefficients, not mobilities. But the theoretical and computational modeling efforts which predict temporal exponents satisfying $3 \leq n \leq 4$ when diffusion in the precipitate phase is very sluggish invariably use mobilities, so it seems worthwhile to calculate the mobilities in the γ and γ' phases for the two temperatures of interest in this work. M is expressed by the equation

$$M = (1 - X)D_{\text{Al}}^* + XD_{\text{Ni}}^*, \quad (17)$$

which is the coefficient of ΦS in Eq. (8); Eq. (17) applies to both the γ and γ' phases. To estimate M for the γ phase, the chemical diffusion coefficients, \tilde{D} , as functions of composition at 898 and 988 K were calculated using the activation energies and pre-exponential factors reported in Table 1 of Watanabe et al. [33]; the EPMA results exhibit less scatter and so were favored in this analysis. To calculate M from \tilde{D} , it is necessary to know the thermodynamic factor Φ . These were obtained using the formula $\Phi = R_g T G''_{m\gamma}$ (R_g is the gas constant) after calculating $G''_{m\gamma}$ using the procedures described in [37], which are based on the thermodynamic model of Ansara et al. [86]. The vacancy wind factor, S , is ignored in these calculations.

The mobilities in the γ' phase were calculated using the data presented in Tables 1 and 2. It was necessary only to calculate D_{Al}^* from the values of D_{Al} shown in the 8th columns using the formula $D_{\text{Al}}^* = D_{\text{Al}}/\Phi$. The mobilities as functions of concentration are shown in Fig. 7. It is immediately evident that the mobility functions used in all the theoretical and computational efforts bear no resemblance whatsoever to the mobilities shown in Fig. 7. In particular, what is lacking physically in all the theoretical and computational work is the variation of M through the γ/γ' interface. It is also evident that the mobility in the γ' phase at both temperatures is ~ 15 times smaller than that in the γ phase. Since the γ/γ' interface is diffuse, it would seem that any model of coarsening in this alloy system that fails to take into account the variation of M through the interface cannot possibly capture the physics of coarsening in Ni-based γ/γ' alloys. It follows that all claims that late-stage coarsening is represented by a temporal exponent satisfying $3 \leq n \leq 4$, specifically because diffusion is interface controlled when M in the minority phase is

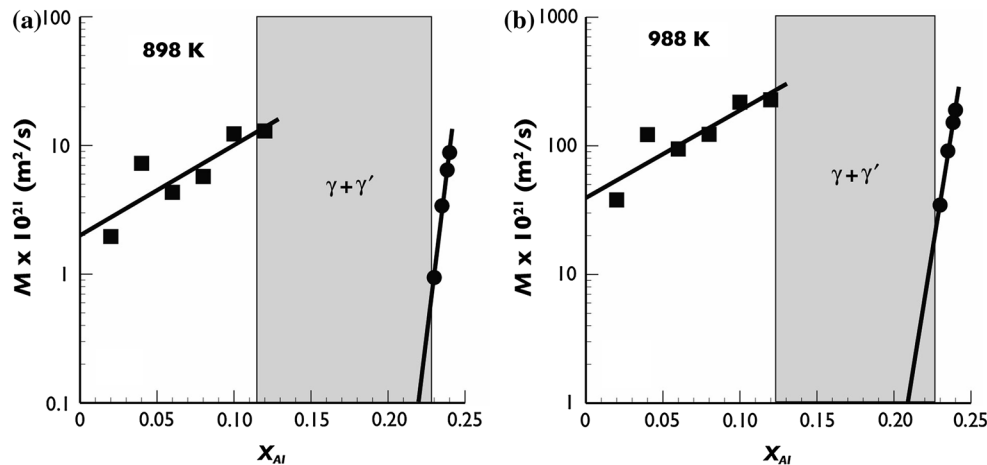


Figure 7 Mobilities in the γ and γ' phases as functions of concentration, X_{Al} , in Ni–Al alloys at two temperatures: **a** 898 K; **b** 988 K. The *filled squares* represent the calculations using the data of Watanabe et al. [33], and the *filled circles* represent the

calculations using the data in Tables 1, 2. The shaded region in each figure represents the 2 phase $\gamma + \gamma'$ region of the Ni–Al phase diagram at 898 and 988 K, respectively. The mobilities are plotted on logarithmic scales.

very sluggish, cannot be correct. In fact, doubts have been raised recently [87–89] about the assertions that interface diffusion control governs late-stage coarsening with mobilities of the type $M^* = 1 - u^2$, even in the sharp interface limit.

What then to make of the claim that the computational results of Sheng et al. [54], and by implication those of Dai and Du [55, 85], are supported by the temporal exponent $n = 3.3$ taken from the data reported by Seidman et al. [84] in Fig. 1 of their paper? Sheng et al. [54] simply used the reciprocal of the slope of the log–log plot of $\langle r \rangle$ versus t ($n = 1/0.3 = 3.33$) to lend credence to their computer simulation results which show that n tends to a value of about 3.35 as M in the precipitate phase approaches zero. It probably does not go without saying, but should, that accepting the validity of temporal exponents obtained from log–log plots of experimental data on coarsening is exceptionally poor practice. To illustrate this, we examine here the same set of data that appears in Fig. 1 of [84]. The original data were published by Sudbrack et al. [90], who tabulated their results, greatly simplifying all subsequent re-evaluation. We analyze here the data on $\langle r \rangle$ versus t from 4 to 1024 h, which are in the coarsening regime (with the possible exception of the datum for 4 h of aging time) and are the same data seen in the log–log plot, Fig. 1 of [84]. There are two paths toward evaluating n in Eq. (2): Method 1 acknowledges the fact that $\langle r_o \rangle$ is simply an essentially

insignificant and ignorable constant of integration that arises from the integration of Eq. (1); Method 2 attributes physical significance to $\langle r_o \rangle$ as a meaningful value of $\langle r \rangle$ at the onset of coarsening. The latter method then requires a multivariate non-linear regression analysis of the same data with $\langle r_o \rangle$, k_T , and n as free parameters. This unfortunately imparts to $\langle r_o \rangle$ a significance that it does not deserve because in fact $\langle r_o \rangle$ is unknown, as is the aging time at the onset of coarsening, and completely needlessly affects the analysis of the data.

In using Method 1, it is necessary only to plot $\langle r \rangle^n$ versus t for different values of n and select the “best” value of n from the plot that produces the best fit to the data, judged from the value of the correlation coefficient R^2 . The data of Sudbrack et al. [90] are plotted this way in Fig. 8a for $n = 2.15$, which provides the best fit of the data. The values of R^2 versus n are inset in this figure. The multivariate non-linear regression analysis of the same set of data produced a value of $n = 2.87$; the data plotted using this value of n are shown in Fig. 8b. Two conclusions can be drawn from the data shown in Fig. 8. The first is that the assertion of Sheng et al. [54] that $n > 3$ when the mobility within the γ' phase is very small is completely unsupported by proper analysis of the data; indeed, the slope of the log–log plot of $\langle r \rangle$ versus t in Fig. 1 of [84] is not only misleading but is also meaningless. The second conclusion is that Method 1 produces a much better fit to the data than Method 2;

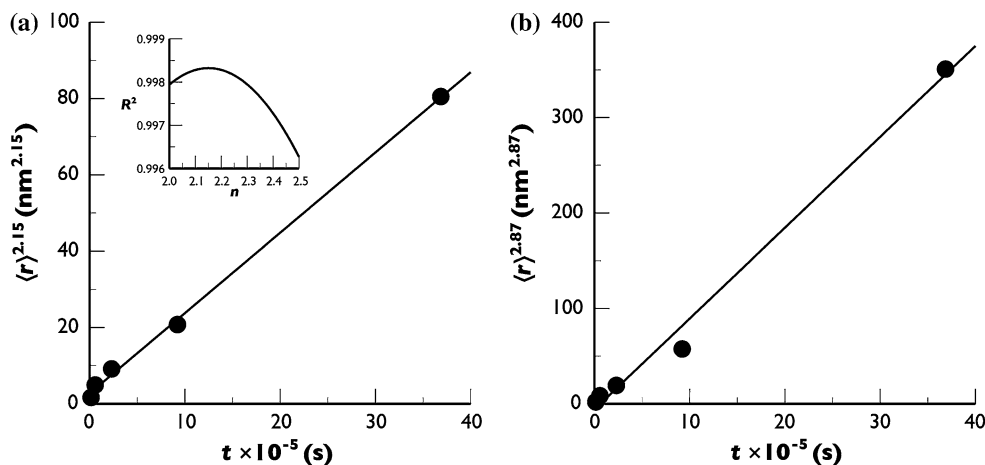


Figure 8 The data of Sudbrack et al. [90] on a Ni–5.2Al–14.2Cr (at.%) alloy aged at 873 K plotted as average particle radius, $\langle r \rangle$, raised to the n th power, versus aging time, t . **a** $n = 2.15$; **b** $n = 2.87$. The correlation coefficient, R^2 , plotted versus n is

this is obvious simply by looking at the two plots in Fig. 8. It is probably not apparent, but the value of k_T obtained using Method 1 is much more meaningful than that obtained using Method 2, simply due to the superior fit to the data.

There are other important points to be made in assessing the results in Fig. 8. Within the framework of the TIDC theory, the most meaningful value of n is obtained from fitting the PSDs, as was done for γ' coarsening in ternary Ni–Al–Cr alloys [39] using PSDs measured by Chellman and Ardell [15] and Jayanth and Nash [91], because in a large set of experimental data on $\langle r \rangle$ versus t for alloys of different composition, plots of $\langle r \rangle^n$ versus t will always produce different values of n . Values of n determined from such plots, exemplified in Fig. 8a, are not necessarily representative of the entire set of data. It is also important to note that the values of R^2 inset in Fig. 8a are all very close to unity, which means that nearly any fit to these data could easily be proclaimed as excellent. This only reinforces the point that n is best determined from fitting the PSDs. Finally, it should be obvious on viewing the data in Fig. 8 that all fits to the data reported by Seidman and his co-workers [43, 90, 92] on the kinetics of growth of γ' precipitates in ternary Ni–Al–Cr alloys are dominated by the value of $\langle r \rangle$ at the longest aging time, which is another reason why all the values of R^2 are close to unity. This is primarily a consequence of inadequate experimental practice, where the aging

shown in inset of (a). The fit in (b) is the result of a multivariate non-linear regression analysis of the same data using Eq. (2) with $\langle r_0 \rangle$, k_T and n as free parameters.

times appear to have been chosen to produce more-or-less equal intervals in log–log plots, such as the one in Fig. 1 of [84]. On the other hand, when aging times are chosen experimentally at approximately equal intervals, similar to the data of Chellman and Ardell [15] and Jayanth and Nash [91], the exponents obtained from measurements of $\langle r \rangle$ versus t are not dominated by the largest value of $\langle r \rangle^n$, irrespective of the magnitude of n , and the rate constants extracted from such data are far more reliable.

Conclusions

The diffusivity of Al in Ni₃Al depends strongly on X_{Al} and is more than an order of magnitude slower than it is in the Ni–Al solid solution matrix. Assuming that the transport of Al through the γ/γ' interface is controlled by the near-precipitate region in the interface, its concentration dependence has been shown to account formally for the non-integer kinetic exponents of γ' particle coarsening in the framework of the TIDC theory. It is therefore possible to fully reproduce all the features and predictions of the TIDC theory without invoking a particle size-dependent interface width. This is consistent with the absence of an effect of f_e on coarsening kinetics in normal Ni–Al alloys and, by implication, in other Ni-based γ/γ' alloys, as well as the considerable effects of f_e on γ coarsening in inverse alloys. Since a detailed

expression for the concentration dependence of the diffusion coefficient does not enter Eq. (16), the magnitude of the interfacial free energy, σ , can be derived as shown previously [37]. The work presented in this paper provides a semi-empirical, but rigorous, explanation for the non-integer temporal exponents that allow the kinetics of coarsening of γ' precipitates in Ni-based alloys, and the PSDs, to be explained by the TIDC theory.

The TIDC theory is at odds with numerous computational and theoretical results that predict temporal exponents exceeding $n = 3$ in systems characterized by sluggish diffusional mobilities in the minority phase. This is rationalized by noting that equations for the mobility used in those theories and computational efforts bear no resemblance at all to real mobilities in Ni–Al alloys and furthermore do not take the mobility through the interface into account. It is shown that when extant data are analyzed properly, there is no experimental support for temporal exponents exceeding $n = 3$.

Acknowledgements

Professor Vidvuds Ozolins, University of California, Los Angeles, provided particularly valuable insights into the thermodynamics and kinetics of transport through diffuse interfaces, as well as the limitations and nuances of phase field modeling. The author is truly grateful to the said professor for his help. Professor Jeffrey J. Hoyt, McMaster University, also provided helpful comments on coarsening and diffusion.

References

- [1] Lifshitz IM, Slyozov VV (1961) The kinetics of precipitation from supersaturated solid solutions. *J Phys Chem Solids* 19:35–50
- [2] Wagner C (1963) Theorie der alterung von niederschlagen durch umlosen. *Z Elektrochem* 65:581–591
- [3] Asimow R (1963) Clustering kinetics in binary alloys. *Acta Metall* 11:72–73
- [4] Sarian S, Weart HW (1966) Kinetics of coarsening of spherical particles in a liquid matrix. *J Appl Phys* 37:1675–1681
- [5] Baldan A (2002) Review-progress in Ostwald ripening theories and their applications to nickel-base superalloys—part I: Ostwald ripening theories. *J Mater Sci* 37:2171–2202
- [6] Ardell AJ (1972) Effect of volume fraction on particle coarsening: theoretical considerations. *Acta Metall* 20:61–71
- [7] Davies CKL, Nash P, Stevens RN (1980) Effect of volume fraction of precipitate on Ostwald ripening. *Acta Metall* 28:179–189
- [8] Marqusee JA, Ross J (1984) Theory of Ostwald ripening: competitive growth and its dependence on volume fraction. *J Chem Phys* 80:536–543
- [9] Brailsford AD, Wynblatt P (1979) Dependence of Ostwald ripening kinetics on particle volume fraction. *Acta Metall* 27:489–497
- [10] Voorhees PW, Glicksman ME (1984) Solution to the multi-particle diffusion problem with applications to Ostwald ripening—II. Computer simulations. *Acta Metall* 32:2013–2030
- [11] Wang KG, Glicksman ME, Rajan K (2005) Length scales in phase coarsening: theory, simulation, and experiment. *Comput Mater Sci* 34:235–253
- [12] Svoboda J, Fischer FD (2014) Generalization of the Lifshitz-Slyozov-Wagner coarsening theory to non-dilute multi-component systems. *Acta Mater* 79:304–314
- [13] Streitenberger P (2013) Analytical description of phase coarsening at high volume fractions. *Acta Mater* 61:5026–5035
- [14] Ardell AJ, Ozolins V (2005) Trans-interface diffusion-controlled coarsening. *Nature Mater* 2005:309–316
- [15] Chellman DJ, Ardell AJ (1974) Coarsening of γ' precipitates at large volume fractions. *Acta Metall* 22:577–588
- [16] Kim D, Ardell AJ (2004) Coarsening behavior of Ni_3Ga precipitates in Ni–Ga alloys: dependence of microstructure and kinetics on volume fraction. *Metall Mater Trans* 35A:3063–3069
- [17] Kim DM, Ardell AJ (2003) Coarsening of Ni_3Ge in binary Ni–Ge alloys: microstructures and volume fraction dependence of kinetics. *Acta Mater* 51:4073–4082
- [18] Meshkinpour M, Ardell AJ (1994) Role of volume fraction in the coarsening of Ni_3Si precipitates in binary Ni–Si alloys. *Mater Sci Eng A* 185:153–163
- [19] Cho J-H, Ardell AJ (1997) Coarsening of Ni_3Si precipitates in binary Ni–Si alloys at intermediate to large volume fractions. *Acta Mater* 45:1393–1400
- [20] Cho J-H, Ardell AJ (1998) Coarsening of Ni_3Si precipitates at volume fractions from 0.03 to 0.30. *Acta Mater* 46:5907–5916
- [21] Kim DM, Ardell AJ (2000) The volume-fraction dependence of Ni_3Ti coarsening kinetics—new evidence of anomalous behavior. *Scr Mater* 43:381–384
- [22] Lund AC, Voorhees PW (2002) The effects of elastic stress on coarsening in the Ni–Al system. *Acta Mater* 50:2085–2098
- [23] Sauthoff G, Kahlweit M (1969) Precipitation in Ni–Si alloys. *Acta Metall* 17:1501–1509

- [24] Harada H, Ishida A, Murakami Y, Bhadeshia H, Yamazaki M (1993) Atom-probe microanalysis of a nickel-base single-crystal superalloy. *Appl Surf Sci* 67:299–304
- [25] Blavette D, Danoix F, Cadel E, Geandier G, Menand A (1999) The utility of tomographic atom probe in interface observation and analysis. *J Phys IV France* 9:113–121
- [26] Sudbrack CK, Isheim D, Noebe RD, Jacobson NS, Seidman DN (2004) The influence of tungsten on the chemical composition of a temporally evolving nanostructure of a model Ni-Al-Cr superalloy. *Microsc Microanal* 10:355–365
- [27] Srinivasan R, Banerjee R, Hwang JY, Viswanathan GB, Tiley J, Dimiduk DM, Fraser HL (2009) Atomic scale structure and chemical composition across order-disorder interfaces. *Phys Rev Lett* 102:086101
- [28] Meher S, Rojhirunsakool T, Hwang JY, Nag S, Tiley J, Banerjee R (2013) Coarsening behaviour of gamma prime precipitates and concurrent transitions in the interface width in Ni-14 at.% Al-7 at.% Cr. *Philos Magn Lett* 93:521–530
- [29] Plotnikov EY, Mao ZG, Noebe RD, Seidman DN (2014) Temporal evolution of the $\gamma(\text{fcc})/\gamma'(L1_2)$ interfacial width in binary Ni-Al alloys. *Scr Mater* 70:51–54
- [30] Mishin Y (2004) Atomistic modeling of the γ and γ' -phases of the Ni-Al system. *Acta Mater* 52:1451–1467
- [31] Ikeda T, Almazouzi A, Numakura H, Koiwa M, Sprengel W, Nakajima H (1998) Single-phase interdiffusion in Ni_3Al . *Acta Mater* 46:5369–5376
- [32] Fujiwara K, Horita Z (2002) Measurement of intrinsic diffusion coefficients of Al and Ni in Ni_3Al using Ni/NiAl diffusion couples. *Acta Mater* 50:1571–1579
- [33] Watanabe M, Horita Z, Sano T, Nemoto M (1994) Electron microscopy study of Ni/ Ni_3Al diffusion-couple interface—II. Diffusivity measurement. *Acta Metall Mater* 42:3389–3396
- [34] Janssen MMP (1973) Diffusion in nickel-rich part of Ni-Al system at 1000 to 1300 °C; Ni_3Al layer growth, diffusion-coefficients, and interface concentrations. *Metall Trans* 4:1623–1633
- [35] Ardell AJ, Kim D, Ozolins V (2006) Ripening of $L1_2$ Ni_3Ti precipitates in the framework of the trans-interface diffusion-controlled theory of particle coarsening. *Z Metallkde* 97:295–302
- [36] Ardell AJ (2010) Quantitative predictions of the trans-interface diffusion-controlled theory of particle coarsening. *Acta Mater* 53:4325–4331
- [37] Ardell AJ (2011) Al- $L1_2$ interfacial free energies from data on coarsening in five binary Ni alloys, informed by thermodynamic phase diagram assessments. *J Mater Sci* 46:4832–4849. doi:10.1007/s10853-011-5395-x
- [38] Ardell AJ (2013) Trans-interface-diffusion-controlled coarsening in ternary alloys. *Acta Mater* 61:7749–7754
- [39] Ardell AJ (2013) Trans-interface-diffusion-controlled coarsening of γ' precipitates in ternary Ni-Al-Cr alloys. *Acta Mater* 61:7828–7840
- [40] Ma Y, Ardell AJ (2007) Coarsening of γ (Ni-Al solid solution) precipitates in a γ' (Ni_3Al) matrix. *Acta Mater* 55:4419–4427
- [41] Ma Y, Ardell AJ (2012) Coarsening of Ni-Ge precipitates in “inverse” Ni_3Ge alloys. *Mater Sci Eng A550*:66–75
- [42] Tsumuraya K, Miyata Y (1983) Coarsening models incorporating both diffusion geometry and volume fraction of particles. *Acta Metall* 31:437–452
- [43] Booth-Morrison C, Zhou Y, Noebe RD, Seidman DN (2010) On the nanometer scale phase separation of a low-supersaturation Ni-Al-Cr alloy. *Philos Magn* 90:219–235
- [44] Ardell AJ (2012) Gradient energy, interfacial energy and interface width. *Scr Mater* 66:423–426
- [45] Al-Kassab T, Kompatscher M, Kirchheim R, Kostorz G, Schoenfeld B (2013) Phase decomposition and ordering in Ni-11.3 at.% Ti studied with atom probe tomography. *Micron* 64:45–51
- [46] Campbell CE (2008) Assessment of the diffusion mobilities in the γ' and B2 phases in the Ni-Al-Cr system. *Acta Mater* 56:4277–4290
- [47] Langer JS, Bar-on M, Miller HD (1975) New computational method in the theory of spinodal decomposition. *Phys Rev A* 11:1417–1429
- [48] Kitahara K, Oono Y, Jasnow D (1988) Phase separation dynamics and external force field. *Mod Phys Lett B* 2:765–771
- [49] Bray AJ (1994) Theory of phase-ordering kinetics. *Adv Phys* 43:357–459
- [50] Bray AJ, Emmott CL (1995) Lifshitz-Slyozov scaling for late-stage coarsening with an order-parameter-dependent mobility. *Phys Rev B* 52:R685–R688
- [51] Emmott CL, Bray AJ (1999) Phase-ordering dynamics with an order-parameter-dependent mobility: the large-n limit. *Phys Rev E* 59:213–217
- [52] Lacasta AM, Hernández-Machado A, Sancho JM, Toral R (1992) Domain growth in binary mixtures at low temperatures. *Phys Rev B* 45:5276–5281
- [53] Kitahara K, Imada M (1978) On the Kinetic equations for binary mixtures. *Suppl Prog Theo Phys* 64:65–73
- [54] Sheng G, Wang T, Du Q, Wang KG, Liu ZK, Chen LQ (2010) Coarsening kinetics of a two phase mixture with highly disparate diffusion mobility. *Commun Comput Phys* 8:249–264
- [55] Dai S, Du Q (2016) Computational studies of coarsening rates for the Cahn-Hilliard equation with phase-dependent diffusion mobility. *J Comput Phys* 310:85–108
- [56] Che DZ, Hoyt JJ (1995) Transient Ostwald ripening in systems with a concentration-dependent diffusivity: I. The LSW limit. *Model Simul Mater Sci Eng* 3:23–34
- [57] Che DZ, Hoyt JJ (1995) Transient Ostwald ripening in systems with a concentration-dependent diffusivity: II.

- Nonzero volume fractions. *Model Simul Mater Sci Eng* 3:35–43
- [58] Morral JE, Purdy GR (1994) Particle coarsening in binary and multicomponent alloys. *Scr Metall Mater* 30:905–908
- [59] Morral JE, Purdy GR (1995) Thermodynamics of particle coarsening. *J Alloys Compd* 220:132–135
- [60] Kuehmann CJ, Voorhees PW (1996) Ostwald ripening in ternary alloys. *Metall Mater Trans* 27A:937–943
- [61] Umantsev A, Olson GB (1993) Ostwald ripening in multicomponent alloys. *Scr Metall Mater* 29:1135–1140
- [62] Numakura H, Ikeda T, Nakajima H, Koiwa M (2001) Diffusion in Ni_3Al , Ni_3Ga and Ni_3Ge . *Mater Sci Eng* A312:109–117
- [63] Ardell AJ (1968) An application of the theory of particle coarsening: the γ' precipitate in Ni-Al alloys. *Acta Metall* 16:511–516
- [64] Manning JR (1967) Diffusion and the Kirkendall shift in binary alloys. *Acta Metall* 15:817–826
- [65] Hancock GF (1971) Diffusion of nickel in alloys based on the intermetallic compound $\text{Ni}_3\text{Al}(\gamma')$. *Phys Stat Sol (a)* 7:535–540
- [66] Bronfin MB, Bulatov GS, Drugova IA (1975) Study of nickel self diffusion in intermetallide Ni_3Al and pure nickel. *Fiz Metal Metalloved* 40:363–366
- [67] Hoshino K, Rothman SJ, Averbach RS (1988) Tracer diffusion in pure and boron-doped Ni_3Al . *Acta Metall* 36:1271–1279
- [68] Frank S, Sodervall U, Herzig C (1995) Self-diffusion of Ni in single and polycrystals of Ni_3Al -A study of SIMS and radiotracer analysis. *Phys Stat Sol (b)* 191:45–55
- [69] Shi Y, Froberg G, Wever H (1995) Diffusion of ^{63}Ni and ^{114m}In in the γ' -phase Ni_3Al . *Phys Stat Sol (a)* 152:361–375
- [70] Hilpert K, Miller M, Gerads H, Nickel H (1990) Thermodynamic study of the liquid and solid alloys of the nickel-rich part of the Al-Ni phase diagram including the AlNi_3 phase. *Berichte Bunsengesell* 94:40–47
- [71] Ikeda T, Numakura H, Koiwa M (1998) A Bragg-Williams model for the thermodynamic activity and the thermodynamic factor in diffusion for ordered alloys with substitutional defects. *Acta Mater* 46:6605–6613
- [72] Cserhati C, Paul A, Kodentsov AA, van Dal MJH, van Loo FJJ (2003) Intrinsic diffusion in Ni_3Al system. *Intermetallics* 11:291–297
- [73] Cserhati C, Szabo IA, Marton Z, Erdelyi G (2002) Tracer diffusion of ^{63}Ni in $\text{Ni}_3(\text{Al}, \text{Ge})$ ternary intermetallic compound. *Intermetallics* 10:887–892
- [74] Belova IV, Murch GE (1998) Test of the validity of the Darken/Manning relation for diffusion in ordered alloys taking the L1_2 structure. *Philos Magn A* 78:1085–1092
- [75] Ma Y, Ardell AJ (2003) The $(\gamma + \gamma')/\gamma'$ phase boundary in the Ni-Al phase diagram from 600 to 1200 °C. *Z Metallkde* 94:972–975
- [76] Calderon HA, Voorhees PW, Murray JL, Kostorz G (1994) Ostwald ripening in concentrated alloys. *Acta Metall Mater* 42:991–1000
- [77] Du Y, Schuster JC (1999) Experimental investigations and thermodynamic descriptions of the Ni-Si and C-Ni-Si systems. *Metall Mater Trans* A30:2409–2418
- [78] Nakajima H, Nonaka K, Sprengel W, Koiwa M (1997) Self-diffusion and interdiffusion in intermetallic compounds. *Mater Sci Eng* A240:819–827
- [79] Cermak J, Rothova V (2002) Ni and Ga diffusion in polycrystalline Ni_3Ga . *Intermetallics* 10:765–769
- [80] Numakura H, Nishi K (2009) Application of mechanical spectroscopy to studies of atomic diffusion in ordered compounds. *Mater Sci Eng* A521–22:34–38
- [81] Komai N, Watanabe M, Horita Z (1995) Interdiffusivity measurements and interface observations using Ni/ Ni_3Ge diffusion couples. *Acta Metall Mater* 43:2967–2974
- [82] Ardell AJ, Nicholson RB (1966) Coarsening of γ' in Ni-Al alloys. *J Phys Chem Solids* 27:1793–1804
- [83] Cahn JW, Hilliard JE (1958) Free energy of a nonuniform system. I. Interfacial free energy. *J Chem Phys* 28:258–267
- [84] Seidman DN, Sudbrack CK, Yoon KE (2006) The use of 3-D atom-probe tomography to study nickel-based superalloys. *JOM* 58:34–39
- [85] Dai S, Du Q (2012) Motion of interfaces governed by the Cahn-Hilliard equation with highly disparate diffusion mobility. *SIAM J Appl Math* 72:1818–1841
- [86] Ansara I, Dupin N, Lukas HL, Sundman B (1997) Thermodynamic assessment of the Al-Ni system. *J Alloys Compd* 247:20–30
- [87] Lee AA, Münch A, Süli E (2015) Degenerate mobilities in phase field models are insufficient to capture surface diffusion. *Appl Phys Lett* 107:081603
- [88] Voigt A (2016) Comment on “Degenerate mobilities in phase field models are insufficient to capture surface diffusion” [*Appl. Phys. Lett.* 107, 081603 (2015)]. *Appl Phys Lett* 108:036101
- [89] Lee AA, Münch A, Süli E (2016) Response to “Comment on ‘Degenerate mobilities in phase field models are insufficient to capture surface diffusion’” [*Appl. Phys. Lett.* 108, 036101 (2016)]. *Appl Phys Lett* 108:036102
- [90] Sudbrack CK, Yoon KE, Noebe RD, Seidman DN (2006) Temporal evolution of the nanostructure and phase compositions in a model Ni-Al-Cr alloy. *Acta Mater* 54:3199–3210
- [91] Jayanth CS, Nash P (1990) Experimental evaluation of particle coarsening theories. *Mater Sci Tech* 6:405–413
- [92] Booth-Morrison C, Weninger J, Sudbrack CK, Mao Z, Noebe RD, Seidman DN (2008) Effects of solute concentrations on kinetic pathways in Ni-Al-Cr alloys. *Acta Mater* 56:3422–3438